JGR Atmospheres

RESEARCH ARTICLE
10.1029/2023JD039235

Converging Findings of Climate Models and Satellite Observations on the Positive Impact of European Forests on Cloud Cover

Luca Caporaso[1,2], Gregory Duveiller[3], Graziano Giuliani[4], Filippo Giorgi[4], Martin Stengel[5], Emanuele Massaro[1], Matteo Piccardo[6], and Alessandro Cescatti[1]

[1]European Commission, Joint Research Centre, Ispra, Italy, [2]National Research Council of Italy, Institute of BioEconomy, Rome, Italy, [3]Max Planck Institute for Biogeochemistry, Jena, Germany, [4]Abdus Salam International Centre for Theoretical Physics, Trieste, Italy, [5]Deutscher Wetterdienst, Offenbach, Germany, [6]Collaborator of European Commission, Joint Research Centre, Ispra, Italy

Abstract Although afforestation is a potential strategy to mitigate climate change by sequestering carbon, its potential biophysical effects on climate, such as regulating surface albedo, evapotranspiration, and energy balance, have not been fully incorporated into climate change mitigation strategies. This is partly due to the challenges associated with modeling the complex bidirectional interactions between vegetation and climate. In this study, we assess the impact of afforestation on low cloud cover using a regional climate model (RCM) and Earth observation data, applying a space-for-time approach to overcome limitations that may arise from comparing satellite and RCM results, such as different background climate conditions or different extents of land cover change. Our results show a consistent increase in low cloud cover in Europe due to afforestation in both datasets (3.71% and 3.56% on average, respectively), but the magnitude and direction of this effect depend on various factors, including location, seasonality, and forest type. These results suggest that afforestation can have important feedbacks on the climate system, and that its biophysical effects must be considered in climate change mitigation strategies. Furthermore, we emphasize the role of the modeling community in developing accurate and reliable approaches to assess the biophysical effects of land cover change on climate.

Plain Language Summary Although forests can help combat climate change by capturing carbon dioxide, we haven't fully considered the potential impact they can have on the climate in terms of biophysical factors such as surface reflectivity, evaporation, and energy balance. This is because it's challenging to accurately model the complex interactions between forests and climate. In this study, we used a regional climate model and Earth observation data to examine how forests affect the amount of low-lying clouds. We used a method that compares satellite and model data to overcome limitations arising from different climate conditions and changes in land cover. Our findings consistently show that forests increase the coverage of low clouds in Europe. However, the specific effects depend on factors such as the location, season, and forest type. These results indicate that forests can have significant impacts on the climate system, and it is important to consider these effects when developing climate change strategies. We also emphasize the need for accurate modeling to better understand how changes in forest cover influence the climate.

Key Points:

- Forests increase the amount of low clouds in Europe
- Forests impact climate beyond carbon sequestration

Supporting Information:

Supporting Information may be found in the online version of this article.

Correspondence to:

L. Caporaso,
luca.caporaso@ec.europa.eu

Citation:

Caporaso, L., Duveiller, G., Giuliani, G., Giorgi, F., Stengel, M., Massaro, E., et al. (2024). Converging findings of climate models and satellite observations on the positive impact of European forests on cloud cover. *Journal of Geophysical Research: Atmospheres*, *129*, e2023JD039235. https://doi.org/10.1029/2023JD039235

Received 11 MAY 2023
Accepted 1 MAY 2024

Author Contributions:

Conceptualization: Luca Caporaso, Gregory Duveiller, Matteo Piccardo, Alessandro Cescatti
Data curation: Luca Caporaso, Graziano Giuliani, Martin Stengel, Emanuele Massaro, Matteo Piccardo
Formal analysis: Luca Caporaso, Emanuele Massaro, Matteo Piccardo
Funding acquisition: Alessandro Cescatti
Investigation: Luca Caporaso, Gregory Duveiller, Graziano Giuliani, Filippo Giorgi, Martin Stengel, Emanuele Massaro, Matteo Piccardo, Alessandro Cescatti
Methodology: Luca Caporaso, Gregory Duveiller, Emanuele Massaro, Matteo Piccardo, Alessandro Cescatti
Project administration: Alessandro Cescatti
Resources: Luca Caporaso, Matteo Piccardo

1. Introduction

Forests are an essential component of the Earth's climate system, playing a vital role in mitigating climate change by absorbing carbon dioxide, an important greenhouse gas contributing to global warming due to its continuously increasing concentration. Indeed, afforestation, which refers here to both reforestation and afforestation, is deemed to be the option with the largest potential for carbon dioxide removal (IPCC, 2019). In addition to their carbon sequestration capabilities, forests also have a direct impact on climate by influencing land-surface properties such as albedo, evapotranspiration (ET), and canopy roughness (Pielke et al., 1998, Davin and de Noblet-Ducoudré 2010). Forests influence the land surface albedo, with darker forested areas absorbing more solar radiation than lighter areas. They also play a crucial role in regulating the global water cycle, releasing water vapor into the atmosphere through ET. The forests' biophysical impacts on climate are increasingly recognized, given their potential role in enhancing or counteracting the climate benefits of land-based carbon sequestration (Anderson-Teixeira et al., 2012; Bonan et al., 2008; Jackson et al., 2008). However, the climate benefits of forests

Software: Luca Caporaso, Gregory Duveiller, Graziano Giuliani, Emanuele Massaro, Matteo Piccardo
Supervision: Luca Caporaso, Gregory Duveiller, Filippo Giorgi, Martin Stengel, Matteo Piccardo, Alessandro Cescatti
Validation: Luca Caporaso, Martin Stengel, Emanuele Massaro, Matteo Piccardo
Visualization: Luca Caporaso, Emanuele Massaro, Matteo Piccardo
Writing – original draft: Luca Caporaso, Matteo Piccardo
Writing – review & editing: Luca Caporaso, Gregory Duveiller, Filippo Giorgi, Martin Stengel, Emanuele Massaro, Matteo Piccardo, Alessandro Cescatti

are still assessed in terms of carbon sequestration potential without considering biophysical impacts, as these are subject to large uncertainties (Lawrence et al., 2022; Perugini et al., 2017).

A relatively little-studied indirect biophysical effect of forests is their ability to modify cloud formation and influence the distribution of precipitation through modifications of atmospheric circulation. This can lead to increased cloud cover, which helps to moderate temperatures and reduce the amount of solar radiation reaching the Earth's surface, further highlighting the importance of forests in mitigating the impacts of climate change. Moreover, the forest canopy can influence the temperature, humidity, and wind patterns driving the formation of clouds, particularly in tropical regions (Bonan, 2008; Laurance et al., 2011). Understanding the complex interactions between forests, clouds, and climate is thus crucial for developing effective strategies to mitigate and adapt to the impacts of climate change. The fact that biophysical effects are still not considered by climate policies contributes to an incomplete evaluation of the climate impacts of anthropogenic land use and land cover change (LULCC) (Duveiller et al., 2020).

The change in the forest area triggers competing cooling and warming effects. Forests are often darker than pastures, agricultural lands, or bear soil (Alton, 2009), and thus deforestation usually leads to an increase in the surface albedo, which results in a cooling effect. On the other hand, the decrease in water evaporation from plants and soils, as well as the reduction in surface roughness caused by a decrease in vegetation canopy, can lead to warming. These biophysical effects can be both direct and indirect, the latter deriving from the modification of the incoming radiation and air temperature due to feedbacks on cloud cover (Boisier et al., 2012; Chen & Dirmeyer, 2016; Davin and de Noblet-Ducoudré, 2010; Pielke Sr et al., 2011). Which mechanism predominates is the result of the non-linear interactions between the direct and indirect effects, and strongly depends on the background climate conditions (Li et al., 2016; Pitman et al., 2011) and latitude (Davin & de Noblet-Ducoudré, 2010). In the temperate and boreal zones of the Northern Hemisphere, the change in the albedo strongly affects the climate, therefore deforestation usually leads to a net cooling effect, especially in boreal regions where snow is present over grassy areas but not over trees (Betts, 2000). As a result of a warming climate, a reduction of radiative effects (Bright et al., 2017) mediated by the decline in snow cover is expected, along with an enhancement of non-radiative cooling due to the increase in ET (Alkama et al., 2022). Conversely, tropical forests are characterized by high ET, and the deep roots of the trees provide for a more effective return of soil moisture to the atmosphere (Fan et al., 2017; Oliveira et al., 2005). In this case, deforestation results in net warming due to the changes in evaporative capacity and surface roughness. An example of indirect effects is the change in cloud cover induced by reduced ET.

Commonly, higher ET fosters the emergence of shallow cumulus clouds (Ek & Holtslag, 2004; Gentine et al., 2013). However, specific atmospheric conditions may accentuate cloud formation and precipitation in areas under low soil moisture conditions (Ek & Holtslag, 2004; Findell & Eltahir, 2003). Observational evidence from Teuling et al. (2017) demonstrates increased cloud cover over western European forests, particularly in the Landes and Sologne regions. Over the same region, Bosman et al. (2019) showed using large eddy simulations that it is an enhancement of sensible heat fluxes that drives cloud cover enhancement over temperate forests. Surprisingly, the same mechanism also influences cloud cover enhancement in large cities (Theeuwes et al., 2019). More recently, Pauli et al. (2022) showed that cloud cover might also be higher under nighttime conditions, and using high-resolution simulations Noual et al. (2023) showed that forest cover and windthrow effects on cloud cover over Landes could be simulated well depending on the choice of parameterizations. Xu et al. (2022) further explored the effects of forests on summer cloud cover across different regions, revealing contrasting impacts and attributing the spatial variation in the sign of cloud effects to sensible heating.

In this study, our main goal is to go a step further in examining the local biophysical implications of a land cover transition over Europe by applying a space-for-time (S4T) substitution approach (Blois et al., 2013) to climate model simulations. In the S4T substitution, in its broadest sense, current spatial phenomena are used to understand and model temporal processes that are otherwise unobservable. Within the S4T approximation, in this work, the difference in forest/herbaceous properties of neighboring pixels serves as a proxy for the temporal signal associated with LULCC. This method assumes that all adjacent land cover pixels share a similar background climate, so that, for example, local Cloud Fractional Cover (CFrC) differences between forests and herbaceous vegetation can be mostly attributed to land cover changes. Here we use a S4T substitution algorithm developed in a previous study (Duveiller et al., 2018a) to CFrC and land fractional cover datasets to quantify the impacts that a complete local transition from forest to grass surfaces would have on the CFrC. We investigate a poorly understood indirect

biophysical effect: how changes in forest cover might alter the overlying cloud regime, which could affect both the energy and water budgets at local to regional scales. Since convective clouds originate in the planetary boundary layer, we specifically focus on low clouds, which are very sensitive to interactions between the land and atmosphere (Rieck et al., 2014). Following a recent study (Duveiller et al., 2021a, 2021b) providing an assessment of this effect on a global scale using satellite remote sensing observations, we conduct a similar study using regional climate model (RCM) simulations. Comparing satellite-based observations with climate models in terms of LULCC and associated biophysical impacts often yields ambiguous results (Chen & Dirmeyer, 2020). Several examples can be found in the literature showing that global climate models and observations lead to conflicting results on the impact of deforestation on summer temperature (Lejeune et al., 2017). It is argued that the inconsistencies between model results and observations are related to problems in parameterization schemes (Findell et al., 2017; Lejeune et al., 2017; Li et al., 2018), differences in the scales adopted (Leite-Filho et al., 2021; Pitman & Lorenz, 2016), differences in background climate conditions (Pitman et al., 2011) or effects that are not properly captured by the models, such as the influence of indirect climate feedbacks that are not detectable using observation-based approaches (Chen & Dirmeyer, 2020). While we acknowledge that land surface models are subject to uncertainty (Chen et al., 2018; Meier et al., 2018), we recognize that *a limitation* of existing comparisons between observations and model simulations is how models and data are compared.

Observational studies are mostly based on the hypothesis that background climate conditions do not change substantially across adjacent land units and therefore changes in surface temperature can be attributed only to LULCC. This S4T analogy has a clear limitation when comparing observed local impacts to model simulations (Chen & Dirmeyer, 2020). First, climate model-based sensitivity studies comparing two separate integrations with and without LULCC do not preserve the background climate because they must necessarily reflect atmospheric feedbacks. Furthermore, observations and model simulations are often characterized by different resolutions, the latter being typically coarser, and this makes the intercomparison problematic, in that the S4T substitution approach may hold only at very fine scales, since non-local effects may be important on coarser scales. To ameliorate this problem we employ RCM simulations at convective permitting resolutions using the same horizontal grid as that of the satellite product employed in this study, and to preserve the climate background, we evaluate the climate model output using a S4T substitution algorithm. To evaluate the performance of the RCM for the European region, we conducted a comparison between the model output and satellite-based datasets. This approach enabled us to assess the accuracy of the model outcomes and identify any potential areas for improvement.

2. Methods

2.1. Retrieving Potential Cloud Fractional Cover Change

The S4T assumes that changes in land cover can explain local variations in CFrC between forests and herbaceous vegetation. While this main hypothesis can be confirmed for surface variables (e.g., temperature), when it comes to atmospheric variables such as clouds, which may move over time, it requires extra assumptions. The approach consists in applying an un-mixing operation over a spatially moving window containing n valid pixels, each pixel characterized by a combination of m values representing distinct land cover type fractions. Over each window, we define the vector $\boldsymbol{y}$ of dimensions $(n \times 1)$, whose element y_i is the CFrC value of the i-th pixel, and n vectors $\boldsymbol{x}_i$ of dimensions $(m \times 1)$, where x_{ij} is the jth land cover type fraction of the ith pixel. Note that each vector $\boldsymbol{x}_i$ contains $m-1$ independent values, because of $\sum_j x_{ij} = 1$. Collecting the vectors $\boldsymbol{x}_i$ as the rows of the matrix $\boldsymbol{X}$ of dimensions $(n \times m)$, we can write:

$$\boldsymbol{y} = \boldsymbol{X}\boldsymbol{\beta} \tag{1}$$

where the vector $\boldsymbol{\beta}$ has dimensions $(m \times 1)$ and collects the coefficients modeling the relationship between y_i and $\boldsymbol{x}_i$. The best β_i values are estimated by the linear least squares method after singular value decomposition (SVD) of $\boldsymbol{X}$, see (Duveiller et al., 2018a, 2018b) for the details. Knowing $\boldsymbol{\beta}$, the value y for the pixel at the center of the local window is calculated as $y = \boldsymbol{w}\boldsymbol{\beta}$, with $\boldsymbol{w}$ any desired combination of land cover types. Then, the change $\Delta y_{A\to B}$ associated with the transition from $\boldsymbol{w}_A$ to $\boldsymbol{w}_B$ combination is calculated as:

$$\Delta y_{A\to B} = y_B - y_A$$

In this study, we concentrate on three transitions: (a) $\Delta y_{HER \to DFO}$ from pure herbaceous vegetation ($w_{HER} = 1$, $w_{j \neq HER} = 0$) to a pure deciduous forest (DFO) ($w_{DFO} = 1$, $w_{j \neq DFO} = 0$), (b) $\Delta y_{HER \to EFO}$ from pure herbaceous vegetation to pure evergreen forest (EFO) ($w_{EFO} = 1$, $w_{j \neq EFO} = 0$), and (c) $\Delta y_{HER \to FOR}$ from pure herbaceous to pure forest, where the sum of DFO and EFO is one while preserving the relative abundances ($w_{DFO} = x_{DFO}/(x_{DFO} + x_{EFO})$, $w_{EFO} = x_{EFO}/(x_{DFO} + x_{EFO})$, and $w_{j \neq DFO, j \neq EFO} = 0$, with x_{EFO}, x_{DFO} observed land cover type fractions for the studied pixel).

The vectors $\boldsymbol{\beta}$ are calculated using a spatial window of 7×7 pixels, each pixel being 5 km, resulting in a squared spatial window of circa 35 km in size. To ensure there are enough values to do the un-mixing over each window, we established that there must be a minimum of 60% of valid values in each window (i.e., removing water pixels) and the number of pixels with different values is a minimum of 40%. In post-processing, the pixels with insufficient local co-occurrence of forests and low vegetation cover (e.g., crops and grasslands) are discharged, the areas where considerable topographical variation occurs within the 7×7 pixel moving window are masked, and the information is aggregated to 0.35° spatial resolution. The operation is applied to all 12 monthly layers of CFrC for each of the 11 years from 2004 to 2014, resulting in a total of 132 maps Δy with a 5 km spatial resolution for each of the three vegetation cover transitions. The post-processing steps of (a) masking all pixels with co-occurrence I_c of the two/three vegetation classes involved in the transition lower than 0.4, (b) removing the potential orographical effects, and (c) aggregating to the coarser spatial resolution of 0.35°, are maintained as discussed in (Duveiller et al., 2018a, 2018b). The co-occurrence in step a is calculated over each window as:

$$I_c = 1 - \frac{\sum_{j=1}^{n} \min\left(\left|\boldsymbol{p}_i - \boldsymbol{q}_j\right| \ \forall\, i \in \{1,2,\ldots,n\}\right)}{\sum_{j=1}^{n} \left|\boldsymbol{q}_j\right|}$$

where $\boldsymbol{p}_i$ is a vector representing in the 2D/3D space the ith pixel of the window, whose components are the two/three land cover types involved in the transition (e.g., $\boldsymbol{p}_i = (x_{i,EFO}, x_{i,DFO}, x_{i,HER})$ for the transition $\Delta y_{HER \to FOR}$), $\boldsymbol{q}_j$ the 2D/3D vector collecting the coordinates of the jth point over a set of n points which are generated equally distributed on the line α passing (1, 0) and (0, 1) in the 2D case, or the plane π passing (1, 0, 0), (0, 1, 0), (0, 0, 1) in the 3D case. $\left|\boldsymbol{q}_i\right|$ indicates the modulus of $\boldsymbol{q}_i$. I_c is maximum when the points $\boldsymbol{p}_i$ coincide.

The space-for-time method would be compromised by the typical translation of topographical features into climate gradients. For this purpose areas with strong elevation gradients are masked out to filter topographic effects. Three factors determine how pixels are masked. Firstly, the standard deviation of the elevation within the local window must not exceed 50 m. Secondly, the difference between the central pixel's mean elevation and the local window's overall mean elevation must not exceed 100 m. Lastly, the difference between the central pixel's and the local window's total standard deviation of elevation must not exceed 100 m with the points $\boldsymbol{q}_i$, that is, all the pixels in the window are characterized by a large presence of the land cover types involved in the transition (i.e., the points $\boldsymbol{p}_i$ are on the α line/π plane), and there is a large variance of the compositional variation (i.e., maximum spatial distribution of the points $\boldsymbol{p}_i$ on the α line/π plane).

Moreover, we addressed the potential impact of water on the S4T performance by treating wetlands as a distinct vegetation cover class when studying transitions from herbaceous vegetation to either evergreen or deciduous forests. Additionally, we accounted for water influence, particularly along coastlines, in our methodology. To minimize this effect, we employed an experimental setup that required more than 60% of the pixels within a moving window to be valid non-water pixels, generating a buffer around coastlines. This ensured that values in these areas, where cloud formation may be dominated by the sea, were ignored. Furthermore, considering the potential influence of window size on the S4T, we set the window size to 7×7 pixels as a compromise between having a sampled area large enough to correctly represent the land cover, and small enough to assume a consistent climate within the window.

2.2. Snow Cover Masking

We mask out the pixels characterized by a snow cover larger than 10% to prevent possible artifacts in Earth observations (EO) datasets due to the potentially incorrect detection of clouds in the presence of snow (Hall et al., 2019). The snow cover is from the level 3 MOD10CM product (Hall & Riggs, 2021), version 6.1, which is

estimated monthly at 0.05° resolution on the full globe. The MOD10CM data are interpolated on a 0.35° grid using a conservative remapping to match the spatial resolution of the S4T results.

2.3. Model

We completed a simulation covering the 11-year period 2004–2014 at convection-permitting spatial resolution over Europe using the non-hydrostatic version of the RCM RegCM5 (Giorgi et al., 2023a). The model is fully coupled with the CLM4.5 land model (Oleson et al., 2013) and is driven at its lateral boundaries in a one-way nesting setup using a 6-hourly time series of sea surface temperature, surface pressure, wind, temperature, and specific humidity on pressure levels from ERA-5 reanalysis at 0.25° resolution (Hersbach et al., 2020).

The atmospheric grid is defined in Cartesian coordinates at 5 km horizontal resolution. It is transformed to geographical coordinates by Lambert conformal conic projection, with the domain centered at 12.25°E and 51.75°N, and 23 vertical sigma levels. Lateral boundary conditions are implemented using an exponential relaxation procedure with a buffer zone width of 40 grid points (Giorgi et al., 1993) without internal nudging. The model uses the Zeng Ocean Air-Sea scheme (Zeng et al., 1998) to parametrize air-sea exchanges, while clouds are explicitly simulated using the Single-Moment 5-class microphysics scheme of the Weather Research and Forecasting model (Skamarock et al., 2008).

For the representation of land surface processes, RegCM5 uses CLM 4.5 (Oleson et al., 2013), which we run using prescribed phenology based on MODIS data (Lawrence & Chase, 2007). In our experiment, we do not consider the contribution of aerosols and gas chemistry. The time step of integration is 30 s and the model output has a bi-hourly frequency. The model is initialized with ERA-5 meteorological fields on 1 October 2003, and the first 3 months (October–December) are treated as a spin-up period, and thus are not considered in the analysis.

2.4. Earth Observation

As reference observation data, we use the Cloud CCI MODIS-Aqua dataset (Stengel et al., 2017). This dataset spans the period 2004–2014 but in contrast to the original dataset (see also https://dx.doi.org/10.5676/DWD/ESA_Cloud_cci/MODIS-Aqua/V002) the monthly data for this study was prepared on 0.05° thus on a finer spatial resolution. The MODIS-Aqua observation time is about 13:30 local time at the Equator, which corresponds well with the peak of cumulus cloud production (Eastman & Warren, 2014). A monthly average was calculated from the daily observations at every pixel. The land cover data used in our study is defined on $0.05 \times 0.05°$ pixels, expressed as fractions of vegetation types (i.e., trees and grasses) and land cover classes (i.e., urban area, bear soil, etc.). They are derived from the Land Cover CCI (ESA, 2017), a set of consistent annual maps describing terrestrial surface cover based on The United Nations Land Cover Classification Scheme at 300 m spatial resolution (Di Gregorio, 2005). This information is aggregated both spatially and thematically using a specifically designed framework (Poulter et al., 2015) to produce maps of general land fractional cover with a spatial resolution of 0.05° to match that of the CFrC data. The procedure is identical to a previous study (Duveiller et al., 2018a).

The variables extracted from the model outputs are cloud area fractions in the atmospheric layers for low (cll), medium (clm), and high (clh) clouds, expressed in percentage. These three cloud variables follow the convention described in the International Satellite Cloud Climatology Project (Rossow & Schiffer, 1991), which divides cloud layers based on cloud top pressure (CTP) into high-($CTP \leq 440$ hPa), mid-(680 hPa $\leq CTP < 440$ hPa), and low-level ($CTP > 680$ hPa). The data are extracted at the peak of convective cloud formation around 2 p.m. (Eastman & Warren, 2014) to prevent topographical effects and limit lateral advection.

The percentage of pixels covered by different plant types is the second input required for the S4T analysis. To minimize possible land cover discrepancies, we grouped the CLM 4.5 vegetation classes following Duveiller et al. (2021a, 2021b), that is, EFO, DFO, savannah (SAV), shrubland (SHR), grassland (GRA), wetland (WET), water bodies (WAT), urban (URB), snow or ice (SNO) and barren sparsely vegetated (BSV) classes. The focus here is on afforestation so we consider only three vegetation classes: herbaceous vegetation, which includes grasses and crops, and the forest vegetation classes (i.e., DFO and EFO).

We made the choice of using a different land cover map for CLM4.5 than for ESACCI for a specific reason. For CLM4.5, we used a fixed map that is typically used in CLM4.5 runs with its usual plant functional types. The reason for this was to minimize any effects on the typical parametrization of CLM4.5 that would be dependent on

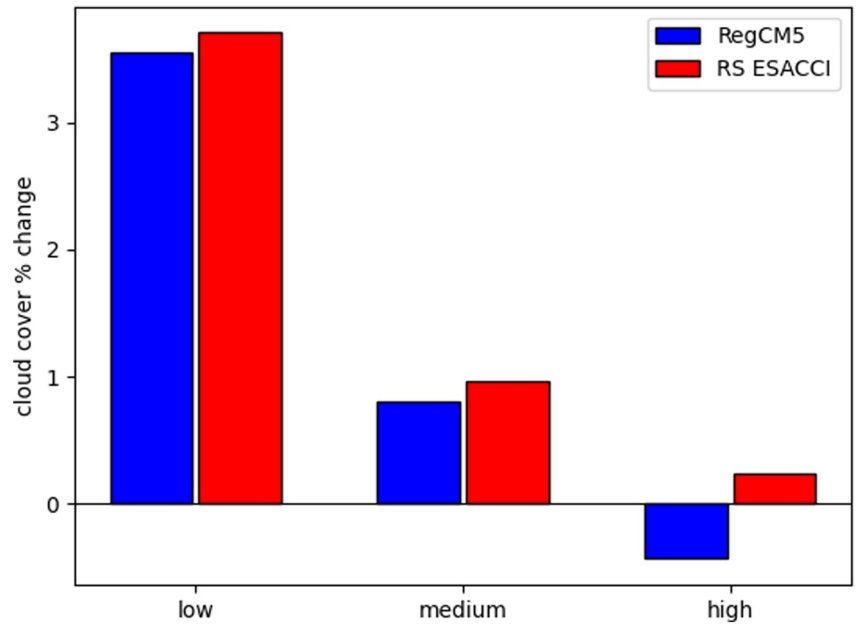

Figure 1. Cloud fractional cover change $\Delta y_{HER \rightarrow FOR}$ following potential afforestation 2004–2014 as derived from RegCM5 and satellite data (Cloud CCI) for low (a), medium (b), and high (c) clouds trees expressed in relative terms to the average cloudiness over every grid cell.

the actual map that is used. However, this map is old and is not necessarily the most accurate representation of the actual land cover. Therefore, we decided to use a more accurate ESA Land Cover map for the study based on ESACCI to ensure the observational data is consistent between cloud and surface. This was a fixed land cover map with a reference year of 2004. We acknowledge that this discrepancy is not ideal, but we considered it was the better way forward. Furthermore, since the space-for-time methodology derives a local sensitivity, it is not crucial that both be consistent with each other, as long as each is internally consistent. To illustrate the potential differences between the two land cover maps, we added Figure S3 in Supporting Information S1, where we have included maps derived from ESACCI for three categories (evergreen, deciduous, and crop/grass) alongside the CLM4.5-derived map. While the main patterns align between the two datasets, differences are noted, such as an overestimation of evergreen coverage by RegCM5 compared to ESACCI, particularly over Russia, Italy, Greece, Croatia, and France, as well as an underestimation of deciduous cover in the same areas. Crop and grass categories are generally well represented, although there is an overestimation in Switzerland and southern France when compared with ESACCI.

3. Results and Discussion

We assess the effect of forest cover on the cloud regime by performing a S4T substitution (see Methods for further details) over a local moving window across the CFrC for the period 2004–2014, both for the RCM outputs and the satellite record. This assumes that the pixels within the moving window share the same climate background states and therefore biophysical differences can be attributed solely to LULCC. By systematically comparing neighboring cloud occurrences, we can isolate in particular the local effect on cloud formation at different levels. In our analysis, the MODIS overpass time of 13:30 was specifically matched with the RegCM5 output spanning from 12:00 to 14:00. This alignment ensures a direct comparison between the observations and model output at the same time of day, enhancing the reliability of our findings.

The CFrC change following potential afforestation for the period 2004–2014 as derived from RegCM5 and satellite data over the entire European domain shows a significant increase in low cloud cover (see Figure 1). Specifically, both RegCM5 and EO show a potential increase in low clouds of 3.56% and 3.71%, respectively, 0.80% and 0.96% for medium clouds, while the results diverge for high clouds, with RegCM5 producing a decrease of 0.43% of high clouds and EO an increase of 0.24%. Therefore, a clear dependency of the signal with altitude is inferred and the results are consistent between the observation and simulation datasets for low and

medium clouds. Notably, it is important to consider that the optimal overpass time for capturing maximal cloud cover contrasts may not align with the MODIS Aqua overpass time of 13:30, particularly in regions like Europe where cloud cover remains relatively high throughout the day (Teuling et al., 2017). Consequently, MODIS data may potentially underestimate the true or average effect due to sampling limitations.

3.1. Inter-Annual Variability of Low, Medium, and High Clouds

The inter-annual variability (IAV) of CFrC change is first investigated using multi-year (2004–2014) monthly scale simulations of RegCM5 low clouds. Figure 2a shows the magnitude and variability of low cloud cover changes associated with afforestation over the domain for each month. On average, the relative increase in low-cloud cover over the European forested areas is comparable in magnitude and variability with the EO data. The model signal shows a relatively constant increase in low cloud cover throughout the year with a minimum in summer and a maximum in winter. In contrast, the EO shows a relative minimum in autumn and a maximum in winter. The analysis of medium (Figure 2b) and high clouds (Figure 2c), confirms that the cloud's response to afforestation is determined mainly by the large-scale patterns rather than the boundary layer processes. As a result, it can be inferred that medium and high clouds have a relatively lower dependency on land surface fluxes. For medium clouds, the model and EO show similar magnitude and variability, with a positive relative impact in CFrC and a maximum in the winter, when also the variability is higher. For high clouds, the correlation with vegetation patterns is very low, with RegCM5 showing a slight decrease over forested areas with a minimum in winter and a maximum in summer, while EO has a moderate increase in all months except January and February.

3.2. Spatial Distribution in Winter and Summer

The spatial changes in CFrC following potential afforestation as derived from RegCM5 and satellite data are shown in Figure 3 for summer (left column, June-July-August period) and winter (right column, December–January–February period). Results are limited to areas with a local co-occurrence of forest and low vegetation cover equal to at least 0.40 and snow cover lower than 10%, and where there is co-occurrence in both model and satellite (scatterplot). As a result, the maps are not spatially continuous. A sensitivity analysis of different combinations of local vegetation cover and snow cover percentage is shown in the Supporting Information S1. Results are presented for low vegetation to forest transitions to illustrate the impact of potential afforestation in the context of a climate mitigation strategy. We find that afforestation induces a relative increase in low clouds over most of the domain. Changes in low cloud cover for summer in the model and EO show similar spatial patterns, with a higher magnitude in EO. In the summer, the clearest positive signal from RegCM5 occurs over central Europe, with relative peaks across Poland, the Czech Republic, Germany, and the France-Spain border. Mixed signals are found in the north of the United Kingdom and Ireland, where the proximity to the sea may complicate matters. According to satellite data, a relative maximum is present over central Europe, with highs over Poland and the Czech Republic as in the RegCM5 simulation, and a weaker signal across Eastern Europe. Therefore, at the local scale, the observations and climate model results agree on the potential cloud cover increase induced by afforestation. Convective clouds are less common in the boreal winter than in summer, and fewer data are available due to the presence of snow. The winter results suggest that both the model and the EO are characterized by a larger variability and a lower correlation than in summer.

3.3. Effect of Different Forest Types

The summer season results show a good level of agreement between model and observations, therefore we decided to explore this result further by investigating the contribution of different forest types on low-cloud formation (Duveiller et al., 2021a, 2021b). We disentangle the forest signal into evergreen and deciduous forests, trying to assess whether the model can capture the differences in CFrC detected by the satellite across different forest species (see Figure 4). Within this context, we concentrate on two transitions: herbaceous vegetation to DFO and herbaceous vegetation to EFO. Our results show that deciduous forests have a comparable signal across model and EO (see left panel of Figure 4), while evergreen forests exhibit a significant divergence in low-level cloud response between RegCM5 and satellite observations (Figure 4 right-side panels). In other words, the model does not distinguish sufficiently well between deciduous and evergreen trees, while the signal from evergreen forests is substantially greater in the EO. A plausible explanation is related to the difference in the partitioning of energy flows (latent vs. sensible), which is too small in the model between the different forest species.

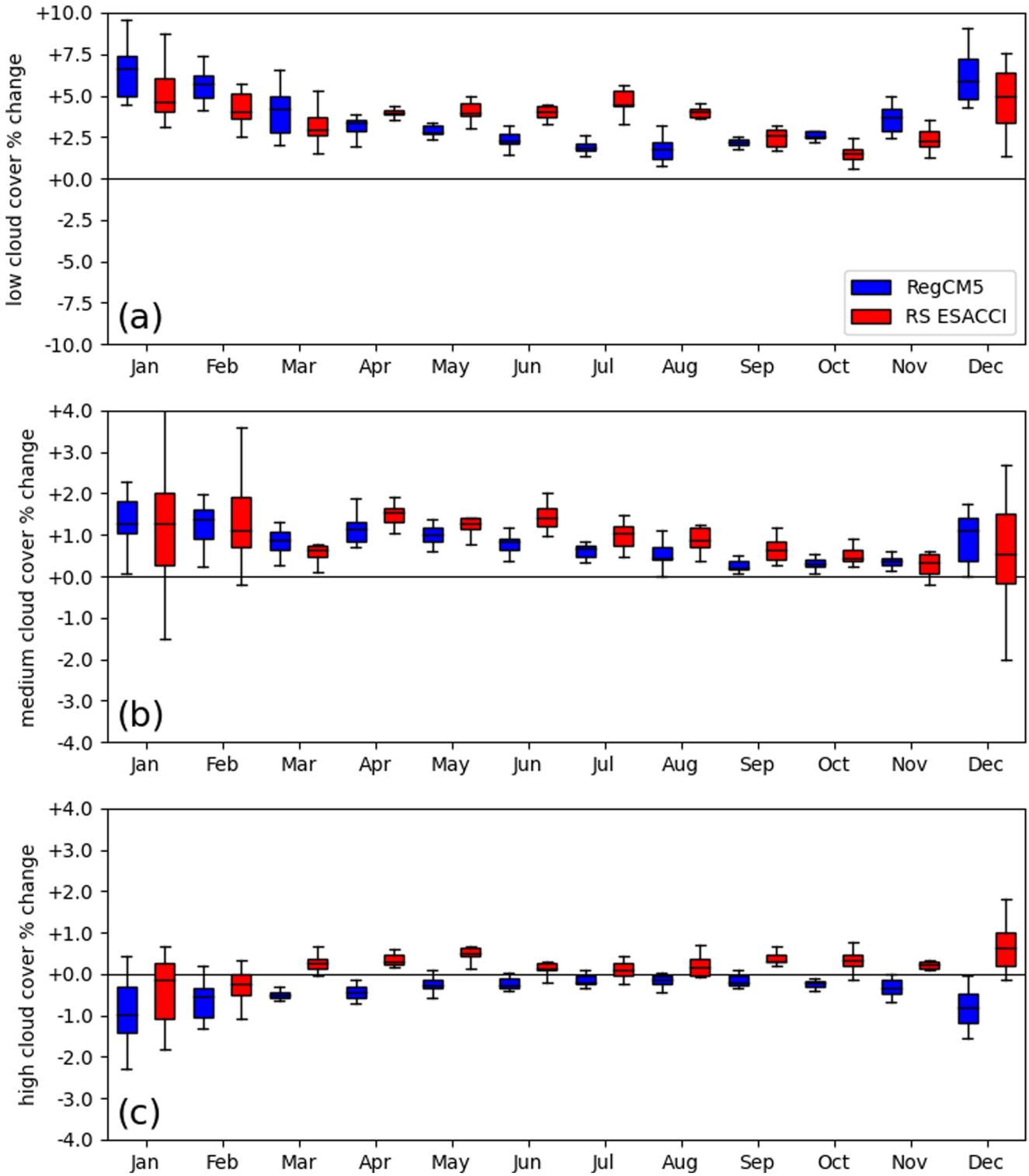

Figure 2. Interannual variability in cloud fractional cover change $\Delta y_{HER \rightarrow FOR}$ following potential afforestation 2004–2014 as derived from RegCM5 and satellite data (Cloud CCI) for low (a), medium (b), and high (c) clouds trees expressed in relative terms to the average cloudiness over every grid cell. Please note that there is a change in scales for the *y*-axis in the panels.

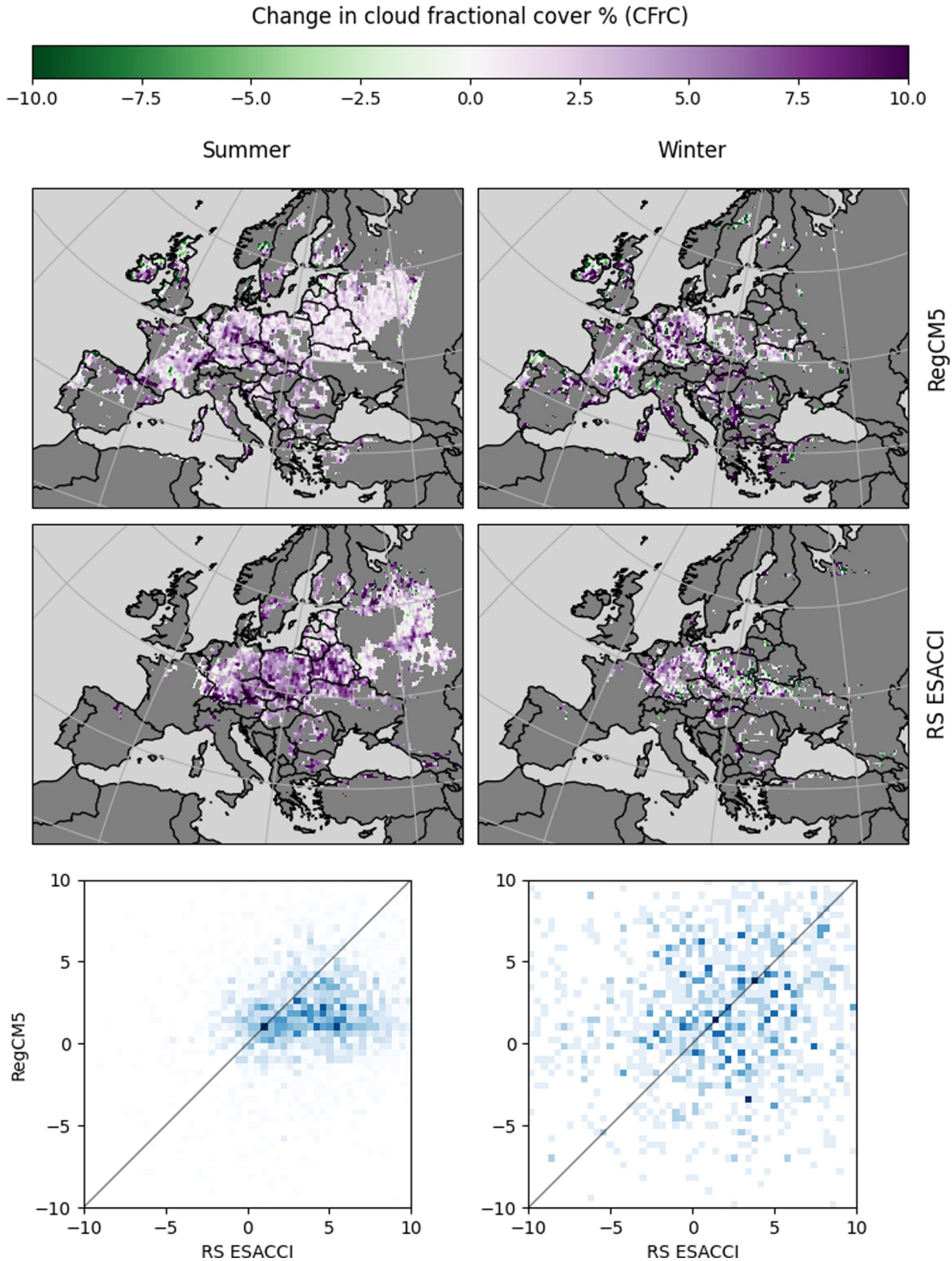

Figure 3. Density plots of changes in low cloud fractional cover $\Delta y_{HER \rightarrow FOR}$ following potential afforestation 2004–2014 in summer (left column) and winter (right column), as derived from RegCM5 and satellite data (MODIS via ESACCI), expressed in relative terms to the average cloudiness over every grid cell. The correlation coefficients between remote sensing ESACCI and RegCM5 for cloud cover change are 0.22 in summer and 0.06 in winter.

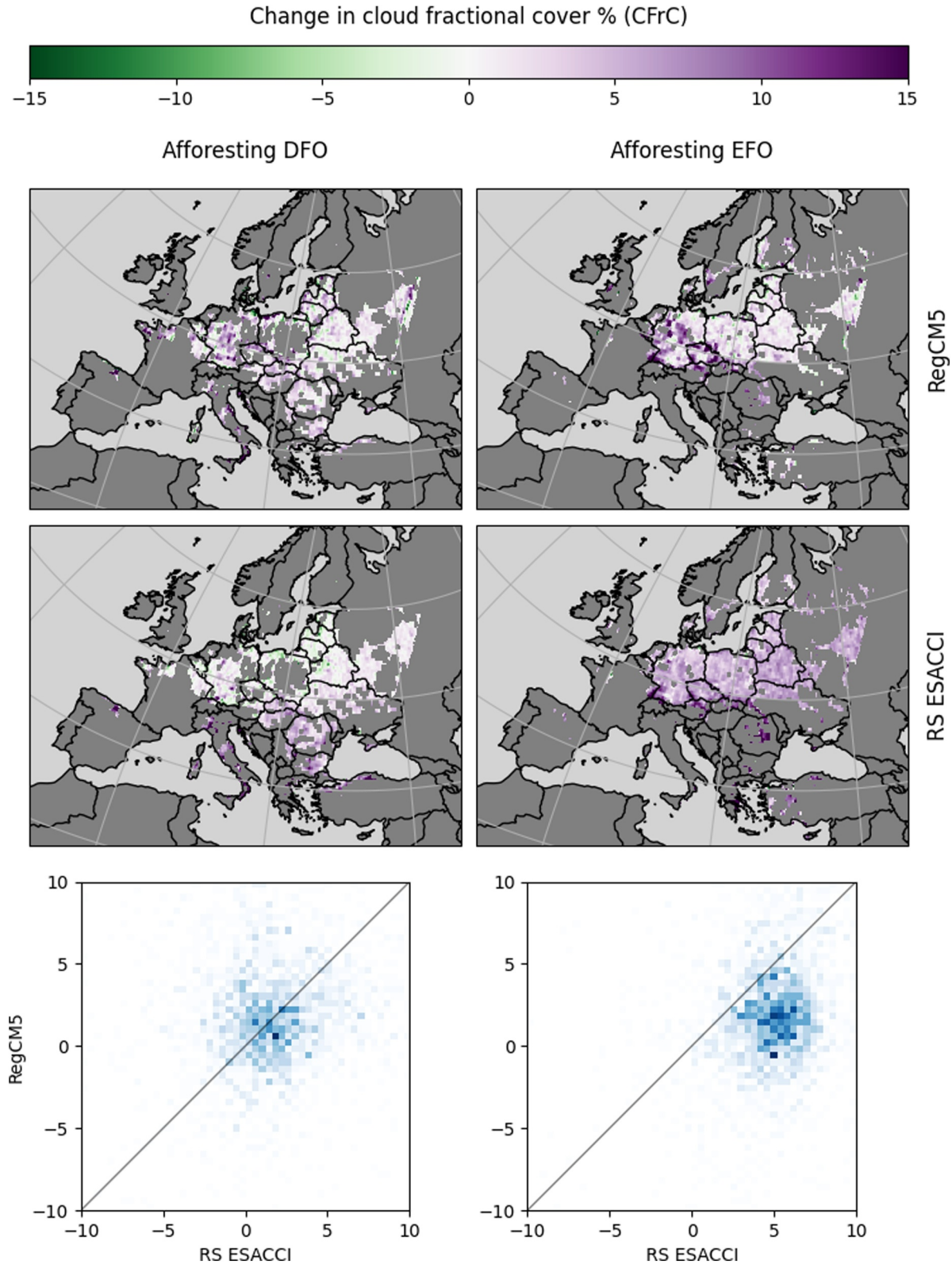

Figure 4. Density plots of changes in low-cloud fractional cover (cloud fractional cover) $\Delta y_{HER \rightarrow DFO}$ and $\Delta y_{HER \rightarrow EFO}$ following potential afforestation 2004–2014 in summer as derived from RegCM5 and satellite data (MODIS via ESACCI), for deciduous (left column) and evergreen (right column) trees expressed in relative terms to the average cloudiness over every grid cell. The correlation coefficients between remote sensing ESACCI and RegCM5 for cloud cover change are 0.24 for deciduous forest and 0.25 for evergreen forest.

4. Conclusion

Current policies underpinning climate mitigation plans, such as the European Green Deal (EC, 2020), rely on afforestation as a possible strategy to increase the potential of carbon dioxide land sink, such as the 3 billion tree planting pledge for 2030 in the European Union. However, beyond the positive consequences of afforestation for carbon storage, its biogeophysical effects should also be considered (De Hertog et al., 2022). In fact, an important piece of climate mitigation strategy options remains unsolved because of our limited understanding of how land cover change and climate interact. One example is our inability to fully picture afforestation's impact on climate.

Using satellite observations and RCM sensitivity simulations at convection-permitting resolutions, framed within the context of a S4T approach we compared responses to afforestation between EO data and model simulations, focusing in particular on local impacts to maximize consistency across the datasets.

Results show that at the local scale, for which the S4T assumption is satisfied, observations and climate model findings agree on the rise in low cloud cover (3.71% vs. 3.56%) that would result from potential afforestation across Europe, thus highlighting the model's capability to simulate cloud formation processes.

Our findings have important implications for the evaluation of climate services provided by forests in Europe. The trees' indirect climate effects via modifications in low cloud formation are aligned with the carbon sequestration's potential to cool the Earth (Duveiller et al., 2021a, 2021b). However, to fully investigate the radiative impact of this effect, a process-based model experiment framework is needed, since some of the cooling induced by the cloud albedo is compensated by the heat greenhouse effect of the clouds (Swann et al., 2012). Additionally, a rise in cloud cover may result in more precipitation (Smith et al., 2023), but it would be hard to quantify the added value of potential afforestation without using a more targeted modeling framework.

In recent years, governments and non-governmental organizations have planned afforestation programs aimed at mitigating the impacts of anthropogenic activities on climate. The broader climatic advantages that forests provide, such as enhancing cloud cover for localized cooling, should be included in climate policies, adding to the hydrological value of forests. We hope that our work will help the scientific community gain a better understanding of the indirect biophysical consequences of afforestation.

Our assessment is driven by model simulations, however, more work and specific sensitivity experiments are needed to disentangle the physical mechanisms involved. The methodology applied here can be easily extended to other model-EO variables, allowing any deficiencies in climate models to be investigated to improve model parameterizations and reduce projection uncertainties.

Data Availability Statement

The RegCM5 model code is available at the website (Giorgi et al., 2023b) https://zenodo.org/record/7548172. The s4t code used in this study, can be found in the following Zenodo repository https://doi.org/10.5281/zenodo.4727822. All the s4t data used in this work have been collected and shared in a public repository (Caporaso et al., 2024) https://zenodo.org/records/10814298 or on request from the first author.

Acknowledgments
This study was supported by the Exploratory Research Project FORBIORES of the European Commission, Joint Research Centre (project number 31520). This research has been supported by the European Research Council, H2020 (USMILE (grant number 855187). Thanks to ICDC, CEN, University of Hamburg for data support.

References

Alkama, R., Forzieri, G., Duveiller, G., Grassi, G., Liang, S., & Cescatti, A. (2022). Vegetation-based climate mitigation in a warmer and greener World. *Nature Communications*, *13*(1), 606. https://doi.org/10.1038/s41467-022-28305-9

Alton, P. (2009). A simple retrieval of ground albedo and vegetation absorptance from MODIS satellite data for parameterisation of global land-surface models. *Agricultural and Forest Meteorology*, *149*(10), 1769–1775. https://doi.org/10.1016/j.agrformet.2009.04.012

Anderson-Teixeira, K. J., Snyder, P. K., Twine, T. E., Cuadra, S. V., Costa, M. H., & DeLucia, E. H. (2012). Climate-regulation services of natural and agricultural ecoregions of the Americas. *Nature Climate Change*, *2*(3), 177–181. https://doi.org/10.1038/nclimate1346

Betts, R. A. (2000). Offset of the potential carbon sink from boreal forestation by decreases in surface albedo. *Nature*, *408*(6809), 187–190. https://doi.org/10.1038/35041545

Blois, J. L., Williams, J. W., Fitzpatrick, M. C., Jackson, S. T., & Ferrier, S. (2013). Space can substitute for time in predicting climate-change effects on biodiversity. *Proceedings of the National Academy of Sciences*, *110*(23), 9374–9379. https://doi.org/10.1073/pnas.1220228110

Boisier, J. P., de Noblet-Ducoudré, N., Pitman, A. J., Cruz, F. T., Delire, C., van den Hurk, B. J. J. M., et al. (2012). Attributing the impacts of land-cover changes in temperate regions on surface temperature and heat fluxes to specific causes: Results from the first LUCID set of simulations. *Journal of Geophysical Research: Atmospheres*, *117*(D12), 1–16. https://doi.org/10.1029/2011jd017106

Bonan, G. B. (2008). Forests and climate change: Forcings, feedbacks, and the climate benefits of forests. *Science*, *320*(5882), 1444–1449. https://doi.org/10.1126/science.1155121

Bosman, P. J., van Heerwaarden, C. C., & Teuling, A. J. (2019). Sensible heating as a potential mechanism for enhanced cloud formation over temperate forest. *Quarterly Journal of the Royal Meteorological Society*, *145*(719), 450–468. https://doi.org/10.1002/qj.3441

Bright, R., Davin, E., O'Halloran, T., Pongratz, J., Zhao, K., & Cescatti, A. (2017). Local temperature response to land cover and management change driven by non-radiative processes. *Nature Climate Change*, *7*(4), 296–302. https://doi.org/10.1038/nclimate3250

Caporaso, L., Duveiller, G., Giuliani, G., Giorgi, F., Stengel, M., Massaro, E., et al. (2024). Converging Findings of Climate Models and Satellite Observations on the Positive Impact of European Forests on Cloud Cover (1.0) [Dataset]. *Zenodo*. https://doi.org/10.5281/zenodo.10814298

Chen, L., & Dirmeyer, P. A. (2016). Adapting observationally based metrics of biogeophysical feedbacks from land cover/land use change to climate modeling. *Environmental Research Letters*, *11*(3), 1–14. https://doi.org/10.1088/1748-9326/11/3/034002

Chen, L., & Dirmeyer, P. A. (2020). Reconciling the disagreement between observed and simulated temperature responses to deforestation. *Nature Communications*, *11*(1), 1–10. https://doi.org/10.1038/s41467-019-14017-0

Chen, L., Dirmeyer, P. A., Guo, Z., & Schultz, N. M. (2018). Pairing FLUXNET sites to validate model representations of land-use/land-cover change. *Hydrology and Earth System Sciences*, *22*(1), 111–125. https://doi.org/10.5194/hess-22-111-2018

Davin, E. L., & Nathalie, de, N.-D. (2010). Climatic impact of global-scale deforestation: Radiative versus nonradiative processes. *Journal of Climate*, *23*(1), 97–112. https://doi.org/10.1175/2009jcli3102.1

De Hertog, S. J., Havermann, F., Vanderkelen, I., Guo, S., Luo, F., Manola, I., et al. (2022). The biogeophysical effects of idealized land cover and land management changes in Earth system models. *Earth System Dynamics*, *13*(3), 1305–1350. https://doi.org/10.5194/esd-13-1305-2022

Di Gregorio, A. (2005). *Land cover classification system (LCCS). Classification concepts and user manual*. Technical Report, Software version 2. FAO.

Duveiller, G., Caporaso, L., Abad-Viñas, R., Perugini, L., Grassi, G., Arneth, A., & Cescatti, A. (2020). Local biophysical effects of land use and land cover change: Towards an assessment tool for policy makers. *Land Use Policy*, *91*, 104382. https://doi.org/10.1016/j.landusepol.2019.104382

Duveiller, G., Filipponi, F., Ceglar, A., Bojanowski, J., Alkama, R., & Cescatti, A. (2021a). Revealing the widespread potential of forests to increase low level cloud cover. *Nature Communications*, *12*(1), 4337. https://doi.org/10.1038/s41467-021-24551-5

Duveiller, G., Filipponi, T., Ceglar, A., Bojanowski, J., Alkama, R., & Cescatti, A. (2021b). GregDuveiller/lulcc-bph-clouds: First Release of lulcc-bph-Clouds (v1.0.0). [Software]. Zenodo. https://doi.org/10.5281/zenodo.4727822

Duveiller, G., Hooker, J., & Cescatti, A. (2018a). The mark of vegetation change on Earth's surface energy balance. *Nature Communications*, *9*(1), 679. https://doi.org/10.1038/s41467-017-02810-8

Duveiller, G., Hooker, J., & Cescatti, A. (2018b). A dataset mapping the potential biophysical effects of vegetation cover change. *Scientific Data*, *5*(1), 180014. https://doi.org/10.1038/sdata.2018.14

Eastman, R., & Warren, S. G. (2014). Diurnal cycles of cumulus, cumulonimbus, stratus, stratocumulus, and fog from surface observations over land and ocean. *Journal of Climate*, *27*(6), 2386–2404. https://doi.org/10.1175/jcli-d-13-00352.1

EC (European Commission). (2020). The European green deal. *Climate Change Energy and Environment*. COM/2019/640 final.

Ek, M. B., & Holtslag, A. A. M. (2004). Influence of soil moisture on boundary layer cloud development. *Journal of Hydrometeorology*, *5*(1), 86–99. https://doi.org/10.1175/1525-7541(2004)005<0086:IOSMOB>2.0.CO;2

ESA. (2017). *Land cover CCI product user guide version 2.0*. European Space Agency. Retrieved from www.esa-landcover-cci.org

Fan, Y., Miguez-Macho, G., Jobbágy, E. G., Jackson, R. B., & Otero-Casal, C. (2017). Hydrologic regulation of plant rooting depth. *Proceedings of the National Academy of Sciences of the United States of America*, *114*(40), 10572–10577. https://doi.org/10.1073/pnas.1712381114

Findell, K. L., Berg, A., Gentine, P., Krasting, J. P., Lintner, B. R., Malyshev, S., et al. (2017). The impact of anthropogenic land use and land cover change on regional climate extremes. *Nature Communications*, *8*(1), 989. https://doi.org/10.1038/s41467-017-01038-w

Findell, K. L., & Eltahir, E. A. B. (2003). Atmospheric controls on soil moisture-boundary layer interactions. Part I: Framework development. *Journal of Hydrometeorology*, *4*(3), 552–569. https://doi.org/10.1175/1525-7541(2003)004<0552:acosml>2.0.co;2

Gentine, P., Ferguson, C. R., & Holtslag, A. A. (2013). Diagnosing evaporative fraction over land from boundary-layer clouds. *Journal of Geophysical Research: Atmospheres*, *118*(15), 8185–8196. https://doi.org/10.1002/jgrd.50416

Giorgi, F., Coppola, E., Giuliani, G., Ciarlo, J. M., Pichelli, E., Nogherotto, R., et al. (2023a). The fifth generation regional climate modeling system, RegCM5: Description and illustrative examples at parameterized convection and convection-permitting resolutions. *Journal of Geophysical Research*, *128*(6). https://doi.org/10.1029/2022JD038199

Giorgi, F., Coppola, E., Giuliani, G., Ciarlo, J., Pichelli, E., Nogherotto, R., et al. (2023b). RegCM-NH V5 Code (5.0.0). [Software]. Zenodo. https://doi.org/10.5281/ZENODO.7548172

Giorgi, F., Marinucci, M. R., Bates, G., & DeCanio, G. (1993). Development of a second generation regional climate model (RegCM2): II. Convective processes and assimilation of lateral boundary conditions. *Monthly Weather Review*, *121*(10), 2814–2832. https://doi.org/10.1175/1520-0493(1993)121<2814:DOASGR>2.0.CO;2

Hall, D. K., & Riggs, G. A. (2021). *MODIS/Terra snow cover monthly L3 global 0.05Deg CMG, version 61. [Indicate subset used]*. NASA National Snow and Ice Data Center Distributed Active Archive Center. https://doi.org/10.5067/MODIS/MOD10CM.061

Hall, D. K., Riggs, G. A., DiGirolamo, N. E., & Roman, M. O. (2019). MODIS cloud-gap filled snow-cover products: Advantages and uncertainties. *Hydrology and Earth System Sciences Discussions*, *123*, 1–23. https://doi.org/10.5194/hess-23-5227-2019

Hersbach, H., Bell, B., Berrisford, P., Hirahara, S., Horányi, A., Muñoz-Sabater, J., et al. (2020). The ERA5 global reanalysis. *The Quarterly Journal of the Royal Meteorological Society*, *146*(730), 1999–2049. https://doi.org/10.1002/qj.3803

IPCC. (2019). In P. R. Shukla, J. Skea, E. Calvo Buendia, V. Masson-Delmotte, H.-O. Pörtner, et al. (Eds.). *Climate change and land: An IPCC special report on climate change, desertification, land degradation, sustainable land management, food security, and greenhouse gas fluxes in terrestrial ecosystems*.

Jackson, R. B., Randerson, J. T., Canadell, J. G., Anderson, R. G., Avissar, R., Baldocchi, D. D., et al. (2008). Protecting climate with forests. *Environmental Research Letters*, *3*(4), 044006. https://doi.org/10.1088/1748-9326/3/4/044006

Laurance, W. F., Camargo, J. L. C., Luizão, R. C. C., Laurance, S. G., Pimm, S. L., Bruna, E. M., et al. (2011). The fate of Amazonian forest fragments: A 32-year investigation. *Biological Conservation*, *144*(1), 56–67. https://doi.org/10.1016/j.biocon.2010.09.021

Lawrence, D., Coe, M., Walker, W., Verchot, L., & Vandecar, K. (2022). The unseen effects of deforestation: Biophysical effects on climate. *Frontiers in Forests and Global Change*, *5*. https://doi.org/10.3389/ffgc.2022.756115

Lawrence, P. J., & Chase, T. N. (2007). Representing a new MODIS consistent land surface in the Community Land Model (CLM 3.0). *Journal of Geophysical Research*, *112*(G1), G01023. https://doi.org/10.1029/2006JG000168

Leite-Filho, A. T., Soares-Filho, B. S., Davis, J. L., Abrahão, G. M., & Börner, J. (2021). Deforestation reduces rainfall and agricultural revenues in the Brazilian Amazon. *Nature Communications*, *12*, 1–7. https://doi.org/10.1038/s41467-021-22840-7

Lejeune, Q., Seneviratne, S. I., & Davin, E. L. (2017). Historical land-cover change impacts on climate: Comparative assessment of LUCID and CMIP5 multimodel experiments. *Journal of Climate*, *30*(4), 1439–1459. https://doi.org/10.1175/jcli-d-16-0213.1

Li, X., Chen, H., Wei, J., Hua, W., Sun, S., Ma, H., et al. (2018). Inconsistent responses of hot extremes to historical land use and cover change among the selected CMIP5 models. *Journal of Geophysical Research: Atmospheres*, *123*(7), 3497–3512. https://doi.org/10.1002/2017JD028161

Li, Y., De Noblet-Ducoudré, N., Davin, E. L., Motesharrei, S., Zeng, N., Li, S., & Kalnay, E. (2016). The role of spatial scale and background climate in the latitudinal temperature response to deforestation. *Earth System Dynamics*, *7*(1), 167–181. https://doi.org/10.5194/esd-7-167-2016

Meier, R., Davin, E. L., Lejeune, Q., Hauser, M., Li, Y., Martens, B., et al. (2018). Evaluating and improving the community land model's sensitivity to land cover. *Biogeosciences*, *15*, 4731–4757. https://doi.org/10.5194/bg-15-4731-2018

Noual, G., Brunet, Y., Le Moigne, P., & Lac, C. (2023). Simulating the effects of regional forest cover and windthrow-induced cover changes on mid-latitude boundary-layer clouds. *Journal of Geophysical Research: Atmospheres*, *128*(13), e2023JD038477. https://doi.org/10.1029/2023jd038477

Oleson, K., Lawrence, D., Bonan, G., Drewniak, E., Huang, M., Koven, C., et al. (2013). *Technical description of version 4.5 of the community land model (CLM)* (p. 420). NCAR Technical Note NCAR/TN-503+STR. https://doi.org/10.5065/d6rr1w7m

Oliveira, R. S., Bezerra, L., Davidson, E. A., Pinto, F., Klink, C. A., Nepstad, D. C., & Moreira, A. (2005). Deep root function in soil water dynamics in cerrado savannas of central Brazil. *Functional Ecology*, *19*(4), 574–581. https://doi.org/10.1111/j.1365-2435.2005.01003.x

Pauli, E., Jan, C., & Teuling, A. J. (2022). Enhanced nighttime fog and low stratus occurrence over the Landes forest, France. *Geophysical Research Letters*, *49*(5), e2021GL097058. https://doi.org/10.1029/2021gl097058

Perugini, L., Caporaso, L., Marconi, S., Cescatti, A., Quesada, B., de Noblet-Ducoudre, N., et al. (2017). Biophysical effects on temperature and precipitation due to land cover change. *Environmental Research Letters*, *12*(5), 053002. https://doi.org/10.1088/1748-9326/aa6b3f

Pielke, R. A., Avissar, R., Raupach, M., Dolman, A. J., Zeng, X. B., & Denning, A. S. (1998). Interactions between the atmosphere and terrestrial ecosystems: Influence on weather and climate. *Global Change Biology*, *4*(5), 461–475. https://doi.org/10.1046/j.1365-2486.1998.t01-1-00176.x

Pielke, R. A., Pitman, A., Niyogi, D., Mahmood, R., McAlpine, C., Hossain, F., et al. (2011). Land use/land cover changes and climate: Modeling analysis and observational evidence Wiley interdiscip. *Reversing Climate Change*, *2*(6), 828–850. https://doi.org/10.1002/wcc.144

Pitman, A., Avila, F., Abramowitz, G., Wang, Y. P., Phipps, S. J., & de Noblet-Ducoudré, N. (2011). Importance of background climate in determining impact of land-cover change on regional climate. *Nature Climate Change*, *1*(9), 472–475. https://doi.org/10.1038/nclimate1294

Pitman, A. J., & Lorenz, R. (2016). Scale dependence of the simulated impact of Amazonian deforestation on regional climate. *Environmental Research Letters*, *11*(9), 094025. https://doi.org/10.1088/1748-9326/11/9/094025

Poulter, B., MacBean, N., Hartley, A., Khlystova, I., Arino, O., Betts, R., et al. (2015). Plant functional type classification for Earth system models: Results from the European space agency's land cover climate change initiative. *Geoscientific Model Development*, *8*(7), 2315–2328. https://doi.org/10.5194/gmd-8-2315-2015

Rieck, M., Hohenegger, C., & van Heerwaarden, C. C. (2014). The influence of land surface heterogeneities on cloud size development. *Monthly Weather Review*, *142*(10), 3830–3846. https://doi.org/10.1175/mwr-d-13-00354.1

Rossow, W. B., & Schiffer, R. A. (1991). ISCCP cloud data products. *Bulletin of the American Meteorological Society*, *72*(1), 2–20. https://doi.org/10.1175/1520-0477(1991)072<0002:icdp>2.0.co;2

Skamarock, W. C., Klemp, J. B., Dudhia, J., Gill, D. O., Barker, D. M., Duda, M. G., et al. (2008). *'A description of the advanced research WRF version 3', Technical Note NCAR/TN-475+STR.* NCAR.

Smith, C., Baker, J. C. A., & Spracklen, D. V. (2023). Tropical deforestation causes large reductions in observed precipitation. *Nature*, *615*(7951), 270–275. https://doi.org/10.1038/s41586-022-05690-1

Stengel, M., Stapelberg, S., Sus, O., Schlundt, C., Poulsen, C., Thomas, G., et al. (2017). Cloud property datasets retrieved from AVHRR, MODIS, AATSR and MERIS in the framework of the Cloud-CCI project. *Earth System Science Data*, *9*(2), 881–904. https://doi.org/10.5194/essd-9-881-2017

Swann, A. L. S., Fung, I. Y., & Chiang, J. C. H. (2012). Mid-latitude afforestation shifts general circulation and tropical precipitation. *Proceedings of the National Academy of Sciences*, *109.3*(3), 712–716. https://doi.org/10.1073/pnas.1116706108

Teuling, A. J., Taylor, C. M., Meirink, J. F., Melsen, L. A., Miralles, D. G., van Heerwaarden, C. C., et al. (2017). Observational evidence for cloud cover enhancement over western European forests. *Nature Communications*, *8*(1), 14065. https://doi.org/10.1038/ncomms14065

Theeuwes, N. E., Barlow, J. F., Teuling, A. J., Grimmond, C. S. B., & Kotthaus, S. (2019). Persistent cloud cover over mega-cities linked to surface heat release. *npj Climate and Atmospheric Science*, *2*(1), 15. https://doi.org/10.1038/s41612-019-0072-x

Xu, R., Li, Y., Teuling, A. J., Zhao, L., Spracklen, D. V., Garcia-Carreras, L., et al. (2022). Contrasting impacts of forests on cloud cover based on satellite observations. *Nature Communications*, *13*(1), 670. https://doi.org/10.1038/s41467-022-28161-7

Zeng, X., Zhao, M., & Dickinson, R. (1998). Intercomparison of bulk aerodynamic algorithms for the computation of sea surface fluxes using TOGA COARE and TAO data. *Journal of Climate*, *11*(10), 2628–2644. https://doi.org/10.1175/1520-0442(1998)011<2628:iobaaf>2.0.co;2